Architecture
Image Studies

Vol.7, Issue 1, pp.2948-2965, 2026
DOI: https://doi.org/10.62754/ais.v7i1.1370

https://journals.ap2.pt/index.php/ais/index

Scan-to-HBIM for the Condition Assessment of a Large Defensive Heritage Complex: The Mers-el-Kébir Fortress (Algeria)

Brahim C.E. LAROUCI[1], Soumia BOUZAHER[2], Haroune BEN CHARIF[3], Sanaa NIAR[4]

Abstract

The integration of Building Information Modeling (BIM) into heritage conservation has improved the documentation, analysis, and management of historic sites, yet its uptake in many developing countries remains limited, with practice still reliant on manual survey and CAD drafting. This study reports a Scan-to-HBIM workflow applied to the Mers-el-Kébir fortress (Oran, Algeria), a multi-period Mediterranean bastioned complex of approximately 54,000 m² documented under the constraints of an active military site within a Ministry of Culture restoration program. A deliberately multi-technique survey combined manual recording, a total-station network, photographic documentation, terrestrial laser scanning (Faro Focus S150 and M70) and ground-penetrating radar (GPR). The TLS campaign acquired 3,000 scans (1,200 with HDR imaging), georeferenced through 31 GPS control stations, over a 13-month period of intermittent, access-restricted windows. Point clouds were registered in Faro Scene, exported in E57 (10–15 mm spacing), processed in Autodesk ReCap, and modeled as a semantically structured HBIM in Graphisoft ArchiCAD; each element was classified, enriched, and exported to the Industry Foundation Classes (IFC) 2x3 schema, the model being validated in Tekla BIMsight. Condition was recorded as a per-space condition assessment and an entity-level crack register; for the North-West Bastion alone, 43 cracks were catalogued and classified by penetration, roughly half being deep or through-going. Recorded degradation and recommended intervention are stored as distinct attribute sets. The principal limitation is the manual modeling effort demanded by irregular historical geometry. Rather than a benchmark, the study contributes a transferable, resource-conscious workflow for the condition-oriented documentation of large, access-restricted defensive heritage.

Keywords: *Scan-to-HBIM; TLS survey; condition assessment; defensive architecture; cultural heritage documentation; Mers-el-Kébir fortress.*

Introduction

Over the past two decades, architectural heritage conservation has been reshaped by digital reality-capture and by the adoption of Building Information Modeling (BIM). The transposition of BIM to historic assets — Heritage (or Historic) BIM (HBIM) — couples accurate three-dimensional geometry with structured, queryable information, supporting more informed restoration planning and asset management (Aricò et al., 2024; Tini et al., 2024).

The Scan-to-HBIM process converts point clouds acquired by TLS, photogrammetry, or structured-light projection into parametric models within a BIM environment (Dell'Amico et al., 2024; Escudero, 2023). Beyond geometry, such models can embed thematic information — material, decay, and historical phasing — that is central to conservation (Aricò et al., 2024; Ferro et al., 2023). Automation and machine learning reduce manual modeling effort and help manage semantically enriched data (Avena et al., 2024; Roman et al., 2023), while confidence indices qualify geometric reliability (Malihi &

[1]Department of Architecture, University Mohamed Khider Biskra BP 145 RP, 07000, Biskra, Algeria. E-mail: brahim.larouci@univ-biskra.dz. ORCID: https://orcid.org/0000-0001-6226-0201 (corresponding author).
[2] Department of Architecture, University Mohamed Khider Biskra BP 145 RP, 07000, Biskra, Algeria E-mail: s.bouzaherlalouani@univ-biskra.dz ORCID: https://orcid.org/0000-0003-4819-0926.
[3] Department of Architecture and Industrial Design, University of Campania Luigi Vanvitelli, Italy
[4] Universidad Politécnica de Madrid, Spain

Bosché, 2024). Difficulties persist in adapting standard BIM libraries to the morphological irregularity of historic fabric (Alshawabkeh et al., 2024).

TLS yields high-resolution data well suited to detecting cracks, cavities, and material loss, and therefore to diagnostics and restoration planning (Nowak et al., 2020; Suchocki et al., 2020); integrating these data into HBIM allows current and historical condition information to be managed together (Chelaru et al., 2024). A substantial strand of the survey-and-representation literature has addressed the semantic dimension of HBIM — how meaning, not only geometry, is encoded so that the model remains intelligible to future conservators (Bianchini et al., 2016; Giannattasio et al., 2020; Quattrini et al., 2018; Valentini et al., 2023). This concern is central here.

These methods are now routine in many countries. In much of the Global South — Algeria included — heritage practice still relies on traditional approaches, constrained by equipment cost, the scarcity of trained personnel, and the absence of standardized protocols. It is against this background that the documentation of the Mers-el-Kébir fortress (Oran) was undertaken, within a Ministry of Culture restoration program, as one of the first large-scale Scan-to-HBIM applications in the country. The fortress is an instructive test case: spatially extensive (≈ 54,000 m²), architecturally heterogeneous across several historical periods, sparsely documented, and — as an active military installation — subject to access restrictions that preclude aerial survey and fragment the survey schedule.

The relevant literature falls into five strands: (i) Scan-to-BIM/HBIM workflows and their automation (Avena et al., 2024; Dell'Amico et al., 2024; Escudero, 2023; Roman et al., 2023); (ii) TLS for heritage documentation and its metric quality (Boardman et al., 2018; Malihi & Bosché, 2024; Pritchard et al., 2017, 2021; Stylianidis & Remondino, 2016); (iii) condition assessment and decay mapping (Aricò et al., 2024; Ferro et al., 2023; Nowak et al., 2020; Suchocki et al., 2020); (iv) semantic enrichment and IFC interoperability (Bianchini et al., 2016; Chelaru et al., 2024; Jerushan et al., 2024; Giannattasio et al., 2020; Ippolito et al., 2023; Quattrini et al., 2018; Valentini et al., 2023); and (v) the documentation of large or access-constrained sites, including defensive heritage (Georgopoulos et al., 2020; Jia et al., 2022; Mancuso & Pasquali, 2016; Sarmiento et al., 2019). The present study sits at the intersection of strands (iii), (iv), and (v).

Three research questions are addressed. (RQ1) To what extent can a TLS-led, multi-technique survey, without UAV (unmanned aerial vehicle) support, capture the geometry and surface condition of a large, multi-period fortress under military constraints? (RQ2) How can condition information be structured within an ArchiCAD-based HBIM — keeping recorded degradation distinct from proposed intervention — so that the model supports conservation decisions rather than mere visualization? (RQ3) What workflow adaptations are required in resource-constrained settings, and what are their limitations? The contribution is methodological and transferable, not a claim of unprecedented accuracy.

The Mers-el-Kébir fortress: context and architecture

Strategic and historical background

Mers-el-Kébir fortress is located northwest of the Algerian Mediterranean coast, 13 km from the city of Oran, 450 km from the capital Algiers, and 250 km from the Spanish coast (Fig.1). The fortress of Mers-el-Kébir has always been coveted throughout history by the great political and military powers of the Mediterranean; the fort's role was to protect the strategically valuable harbor of Mers-el-Kébir (Arabic for the Great Harbor), which was considered in medieval and modern ages as one of the largest natural harbors in the western Mediterranean. Controlling the fortress and the port meant controlling the maritime exchanges between East and West and the ability to house a large war fleet (Cámara, 2010).

Figure 1. Situation of Mers-el-Kébir on the Algerian coast. *(Source: Google Maps, 2024.)*

The citadel of Bordj el Marsa was built in the 14th century by the Mérinide Sultan Abou l'Hassan, in the exact location as the current fort of Mers-el-Kébir, more specifically on the upper part of the peninsula, surrounded by a solid wall with square towers, made with adobe (Pestemaldjoglou, 1940). It has been subsequently modified over the centuries, mainly by the Spanish, who seized the fortress in 1505. In 1514, the engineer Diego de Vera made the first reform project to reduce the defensive area and the number of soldiers needed to protect the fort, as much as to improve the control of the fortress access from the harbor side by incorporating a bastioned circular tower, a ditch, and a wall (De Castro, 2004). However, the essential reform started in 1564 by the engineer Juan Bautista Antonelli (Fig.2), who designed a new fortification according to the rules of 16th-century military engineering based on four important bastions. In that same year, he proceeded to demolish the medieval Islamic fortress, except for a reduced wall section used in constructing the land front (De Castro, 2004).

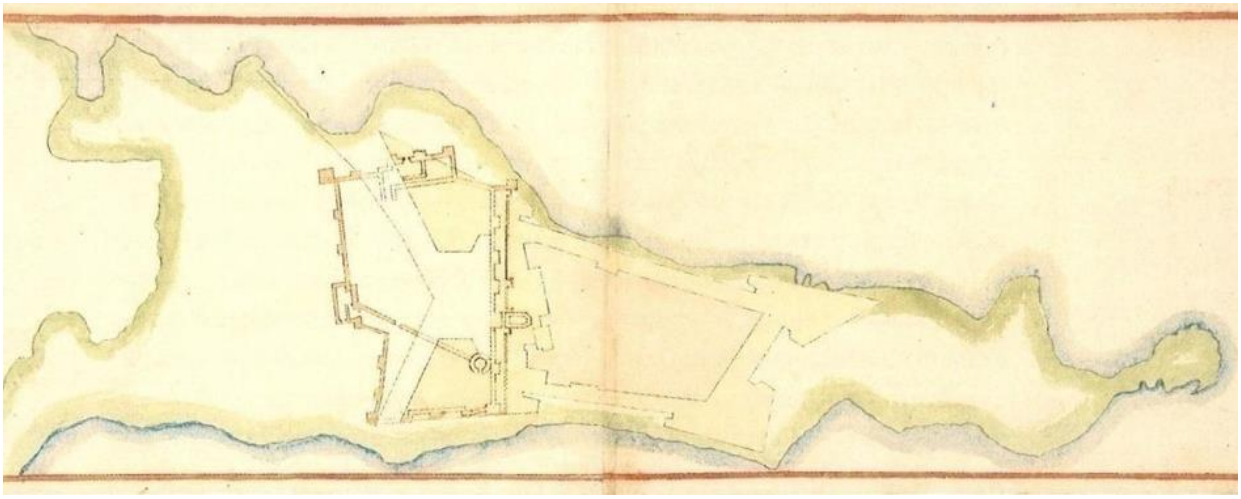

Figure 2. Implantation of Antonelli's bastioned fortification reusing a wall of the Islamic citadel. *(Source: Leonardo Turriano, 1598; after Cámara, 2010.)*

In 1574, the engineer Vespasiano Gonzaga worked on improving the defense with a system of Scissor on the seaside to enlarge the fortification's capacity. This part of the fortress will be called "the fortification of the Calvario"; residences, barracks, and tanks were built within its enclosure. (De Castro, 2004). Two years later, it is the engineer Giovani Giacomo Paleari Fratino, more known as El Fratin, who came up with a new reform to cover the landfront and ensure better protection on the side of the mountain thanks to the projection of a new Ravelin (Cámara, 2010). Although, there have been no significant modifications to the plan of the fort since this period, even if several reinforcements, enlargements, and additions have been made throughout the centuries.

In 1792, the fort was taken over by the Ottomans, then in 1830 by French colonization (Fig.3). Mers-el-Kébir became one of the most important fortresses in the Mediterranean. The importance of its study lies on the stratification of several historical periods from the Islamic fort to the modern one, which implies a challenging continuous adaptation of the construction to the development of artillery. In this sense, some technical solutions have been the subject of important discussions and debates between

military engineers to find the optimal defensive option. Some of these solutions will be used in future fortifications worldwide, as many of them were imported from foreign forts. Mers-el-Kébir played a crucial role in the exchange of techniques and knowledge between engineers. Moreover, the fortress allows us to understand better the political and military stakes that Mers-el-Kébir had, as well as the role it played in the history of the world, from the Middle Ages to World War and beyond.

Figure 3. The fortress of Mers-el-Kébir in 1751. *(Source: Vincennes Historical Archives Centre.)*

Architectural description of the complex

The fortress occupies the promontory as a coherent defensive landscape rather than a single building. Its principal entities are: a corps de place — the enceinte of curtain walls (courtines) enclosing the central place d'armes, with four angle bastions (the two eastern ones left unfinished); a detached, V-shaped demi-lune (ravelin) set on the rock behind a glacis and separated from the body by a ditch; and, downslope, an esplanade of annex buildings and a perimeter of batteries and bunkers around the peninsula and jetty. Characteristic members include orillons shielding the bastion flanks, échauguettes (bartizans) on corbels, chemins de ronde, and parapets pierced by cannon embrasures (canonnières) and loopholes (meurtrières).

The significance of the site — and of its restoration — lies in this stratified, continuously adapted military landscape: successive Marinid, Spanish, Ottoman, and French interventions produced heterogeneous fabric (rubble and ashlar masonry, vaults, rock-cut works) shaped by the evolving demands of artillery. That heterogeneity, the harsh marine environment, and restricted access together justify a high-fidelity digital record as the basis for conservation.

Materials and methods

The documentation was produced by the GAMAP group within the Ministry of Culture restoration program, with BIM collaboration with Art Graphique et Patrimoine (AGP, Paris). Rather than a single technique, a deliberately integrated survey was deployed — manual recording, a total-station network, photographic documentation, TLS, GPS georeferencing, and GPR subsurface prospection (Figure 4; Figure 5). TLS (Faro Focus S150 and M70) was primary. UAV photogrammetry, although desirable for roofs and sea-facing facades, was prohibited by military regulation; consequently no UAV data were acquired or processed, and that coverage was compensated from adjacent TLS and archival sources.

Terrestrial photogrammetry was judged of limited added value for a sparsely ornamented defensive structure.

Figure 4. Division of the fortress into survey entities, used consistently across all phases. *(Source: GAMAP)*

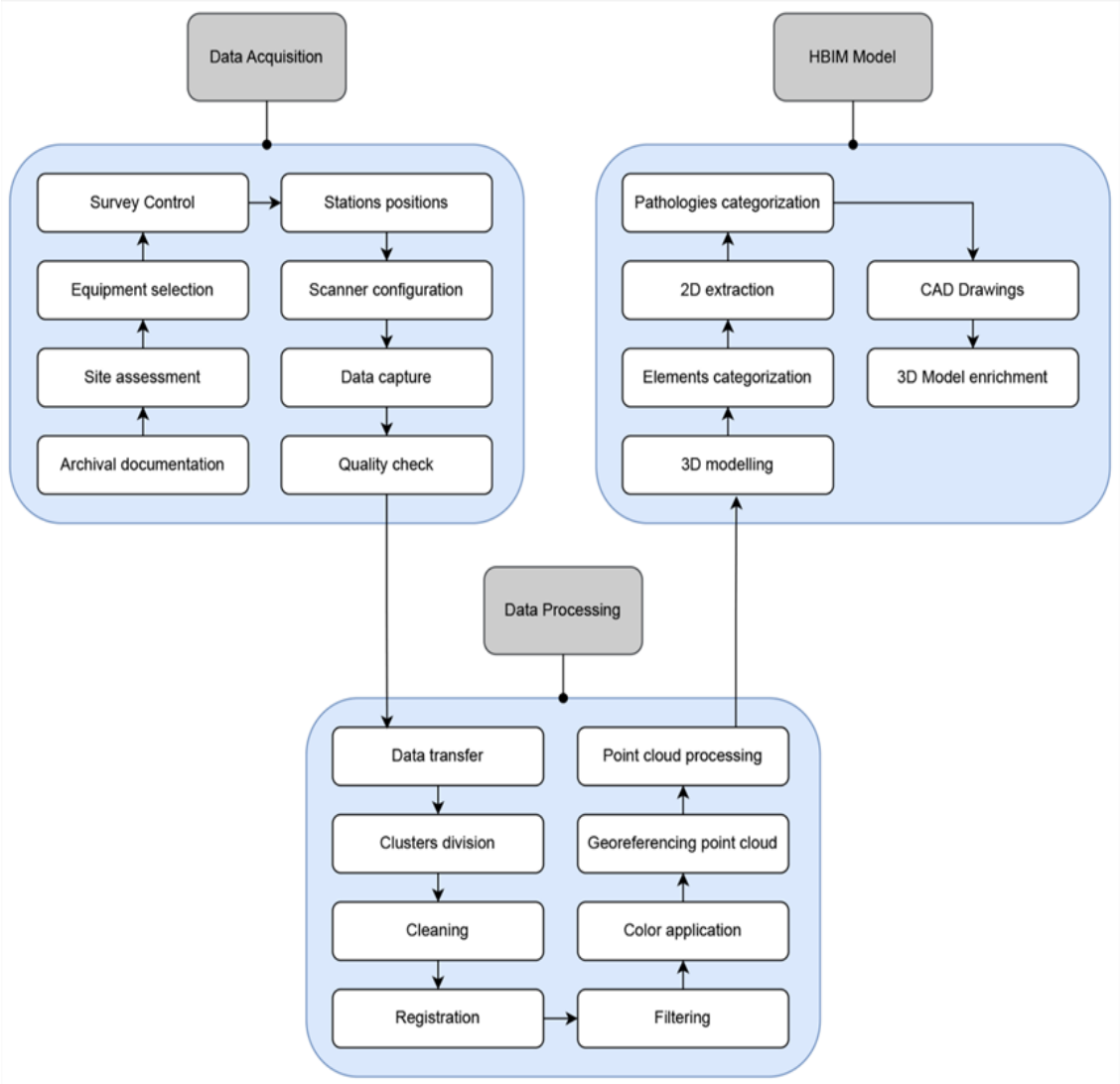

Figure 5. Overall Scan-to-HBIM workflow, from acquisition through condition assessment and IFC export.

Survey control and parameters

Because cloud-to-cloud registration alone accumulates drift across a site of this size, the survey was controlled by a total-station network and 31 GPS control stations distributed across the fortress, to which the entities and the final model were tied. This directly answers the concern that a topographic network is superfluous here: on the contrary, it is what bounds error propagation and provides a common datum. Table 1 summarizes the pipeline and Table 2 the parameters.

Table 1. Stage-by-stage summary of the integrated workflow.

Stage	Input	Tool	Process	Output
Control & georef.	Site; ground control points	Total station; 31 GPS stations	Control network; georeferencing	Reference frame
TLS acquisition	Site geometry	Faro Focus S150 / M70	360° scans, HDR	3,000 scans (1,200 HDR)
Registration	Raw scans; targets/spheres	Faro Scene	Auto cloud-to-cloud + target-based; visual check	Registered clouds

Stage	Input	Tool	Process	Output
Export	Registered clouds	Faro Scene; ReCap	Cleaning; decimation; ortho-images	E57 (10–15 mm); orthophotos; WebShare
Modeling	Point cloud	ArchiCAD	Parametric & custom modeling by entity	HBIM model
Condition	Orthophotos; WebShare	AutoCAD; ArchiCAD	Sanitary assessment; crack register; coding	Condition data
Enrichment / export	Model + condition	ArchiCAD; IFC; Tekla BIMsight	IDs, IFC classes, property sets; validation	Enriched IFC 2x3 model
Subsurface	Ground	MALA ProEx GPR (250/500 MHz)	10 profiles; filtering	Radargrams; anomaly map

Table 2. Acquisition and processing parameters

Parameter	Value
Site area	≈ 54,000 m²
Scanners	Faro Focus S150 (±1 mm) and M70 (±3 mm)
Scan resolution / quality	External 1/2 – 3× – HDR – Large indoor spaces: 1/4 or 1/5 – 4× - Color ON
Total scans / HDR scans	3,000 / 1,200
Control / georeferencing	Total-station network + 31 GPS control stations
Registration software	Faro Scene (cloud-to-cloud + targets/spheres)
Point-cloud export	E57, 10–15 mm point spacing, < 5 GB per set
Modeling / enrichment	Graphisoft ArchiCAD
IFC schema; validation	IFC 2x3; validated in Tekla BIMsight
Subsurface prospection	GPR MALA ProEx, 250 & 500 MHz, 10 profiles
Survey campaign	11 Mar 2018 – 17 Apr 2019 (≈ 13 months, access-restricted)

Survey campaign and access constraints

Because the fortress is an active military installation, access was granted only in intermittent windows, and the survey was organized sector by sector accordingly. The 3,000 scans were therefore distributed across approximately 119 field-days over thirteen months (11 March 2018 – 17 April 2019), an average of about 25 scans per field-day (Table 3). This explains what might otherwise look anomalous: the scan total reflects a long, fragmented, access-restricted campaign — not an implausibly intense few weeks.

Table 3. Survey-campaign timeline by sector. Field days are approximate; some sectors were surveyed concurrently with two scanners.

Sector	Access windows (2018–2019)	Field-days
Demi-lune	11–15 Mar; 9–14 Oct; 24–25 Dec 2018; 7 Feb; 3, 16 Apr 2019	≈ 16
Bastion Nord & Courtine Ouest	3–8 Sep; 15–25 Oct; 17–25, 31 Dec 2018; 1, 21–22 Jan; 5–11 Feb; 3, 15, 17 Apr 2019	≈ 34

Sector	Access windows (2018–2019)	Field-days
Bastion Sud-Ouest	8–11 Sep; 8–9 Oct; 11 Dec 2018; 10, 13–22, 26 Jan; 4–5 Feb; 1–3, 15 Apr 2019	≈ 23
Place d'armes	10–29 Sep; 1–2, 11–15 Oct; 12 Dec 2018; 30 Jan; 3–4, 9–11 Feb 2019	≈ 24
Vaulted casemates & the point	9–17, 27 Sep; 30 Sep–7 Oct 2018; 3, 5–10 Feb 2019	≈ 22
Whole campaign	11 Mar 2018 – 17 Apr 2019 (intermittent, access-restricted)	≈ 119

Data acquisition and entity division

The project opened with manual recording, archival research, and on-site reconnaissance, which informed the division of the fortress into survey entities (Figure 4) — a division retained through every later phase. Station placement followed scanner range, required detail, and object configuration (Boardman et al., 2018; Pritchard et al., 2017), maximizing overlap; connecting stations linked indoor and outdoor spaces, and a 360° HDR coverage met the requirement for web-based visualization.

Registration and point-cloud processing

Scans were assembled in Faro Scene by automatic cloud-to-cloud matching supported by spheres/targets and constrained by the total-station and GPS control, with visual inspection of each assembly (critical for spiral stairs and confined casemates). Noise was reduced and moving objects clipped before export to E57 at 10–15 mm spacing (sets under 5 GB), with a denser variant and 3D views for visualization (Figure 6); the cloud also underpinned 3D extraction in Autodesk ReCap.

Registration quality is reported in Table 4 as defined statistics, distinguishing the cloud-to-cloud residual from the error at independent check points.

Table 4. Registration quality.

Registration metric	Indoor	Outdoor
Mean cloud-to-cloud residual	3 mm	10 mm
Maximum residual	5 mm (measured)	15 mm
Standard deviation	1.5 mm	5 mm
Control framework	Total station + 31 GPS stations	Total station + 31 GPS stations
Check-point residual (RMS)	8–12 mm	10–15 mm

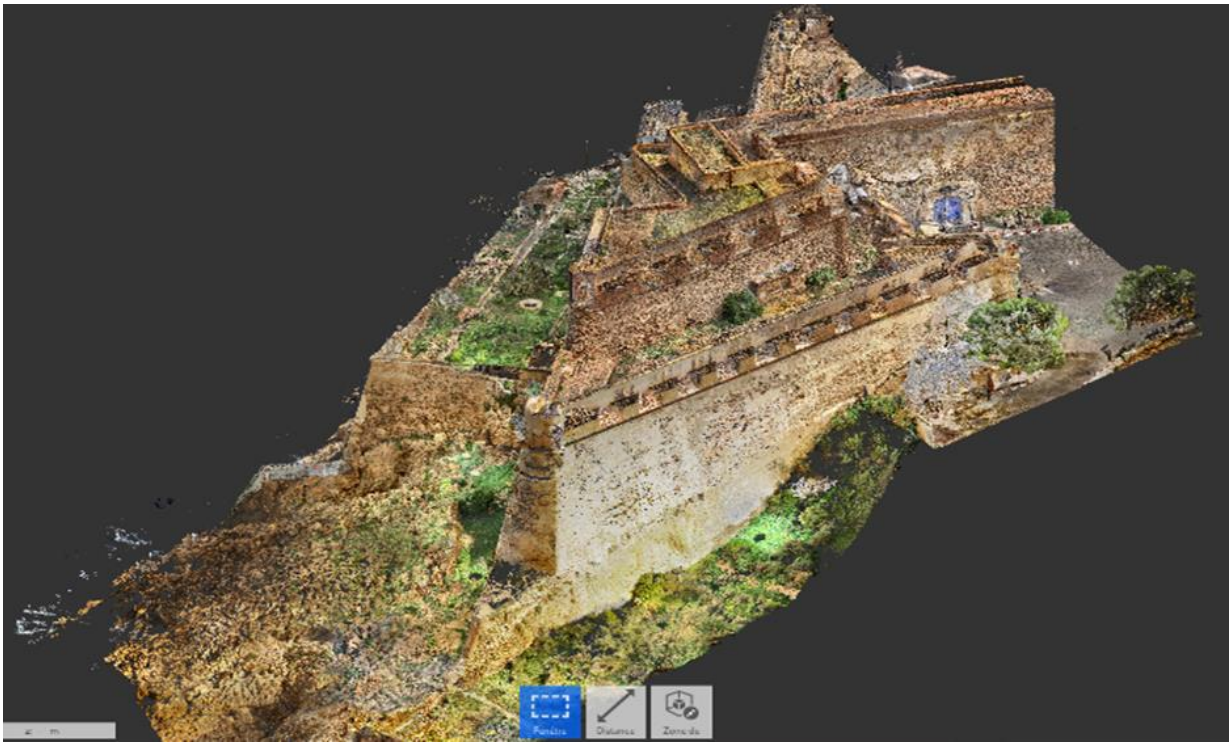

Figure 6. Registered point cloud visualized in Autodesk ReCap.

Subsurface prospection (GPR)

To investigate suspected buried spaces, a ground-penetrating-radar campaign (MALA ProEx; 250 and 500 MHz shielded antennas) was carried out. Ten profiles (four longitudinal, six transverse) were acquired; because the ground proved conductive, the 500 MHz antenna was preferred, giving an investigation depth below ~3 m. After standard filtering (DC removal, mean-trace subtraction, finite-impulse-response (FIR) band-pass, time-gain), two interconnected anomalies at roughly 1 m depth near the center of the site were interpreted as a probable buried vault, recommended for verification. This subsurface dimension distinguishes the survey from routine scan-then-model practice and feeds conservation risk assessment.

HBIM modeling

The light cloud was imported into Graphisoft ArchiCAD — chosen for its wide local adoption — as the modeling base, while verification and measurement used the denser cloud in ReCap and the WebShare viewer's 360° imagery (Figure 7). Each element was built with the proper tool, placed on the correct layer, and assigned a unique identifier and IFC class (Figure 8); modeling mirrored the entity division so operators could work in parallel (Figure 9).

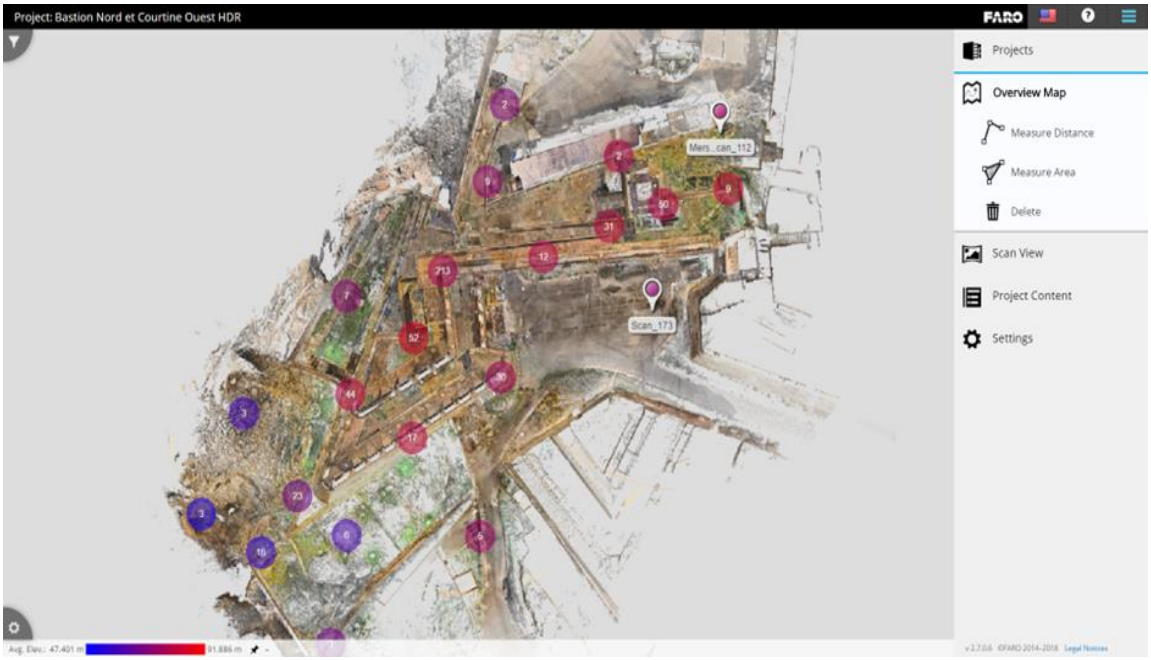

Figure 7. WebShare viewer of the North-West Bastion, used for verification and measurement.

The modeling specification followed the Level of Geometry, Level of Accuracy, and Level of Information (LOG/LOA/LOI) framework (Brumana et al., 2019). The model was produced at LOG 200–300 — an architectural-scale geometry consistent with the 10–15 mm point cloud — with a model-to-cloud tolerance of ±2–3 cm, and an LOI comprising identity, material, historical phase, condition, and recommended intervention. Complex forms — the rock substrate, mouldings, deformed vaults and scarps — were modeled as custom objects.

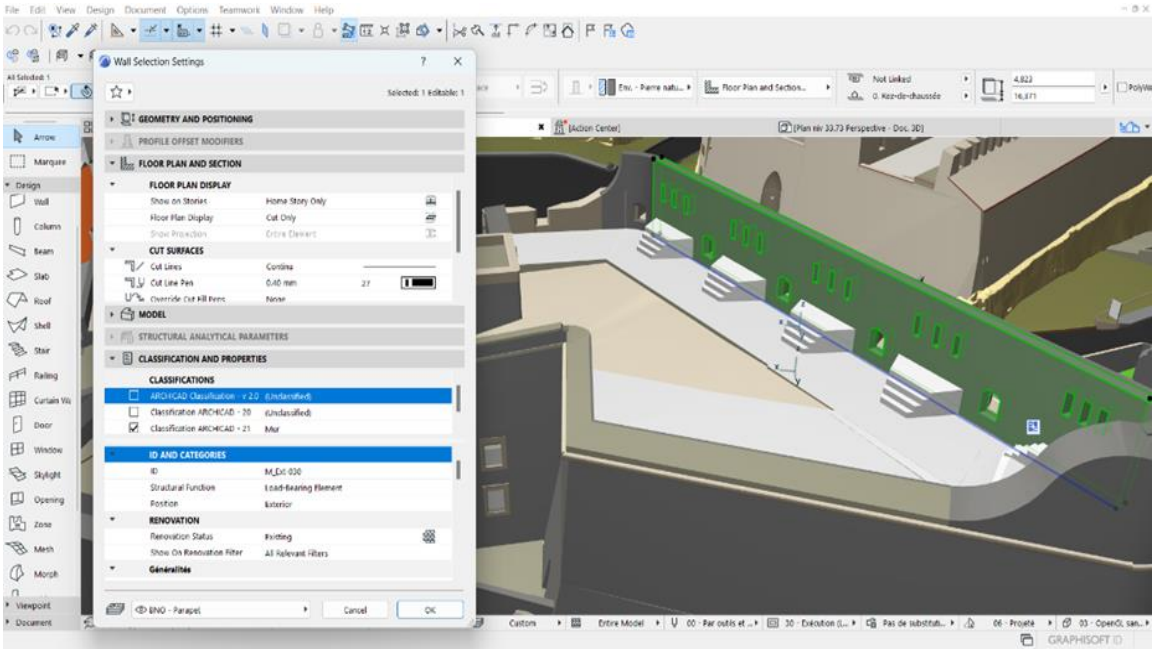

Figure 8. Enrichment of an architectural element in ArchiCAD: geometry linked to identifier, IFC class, and properties.

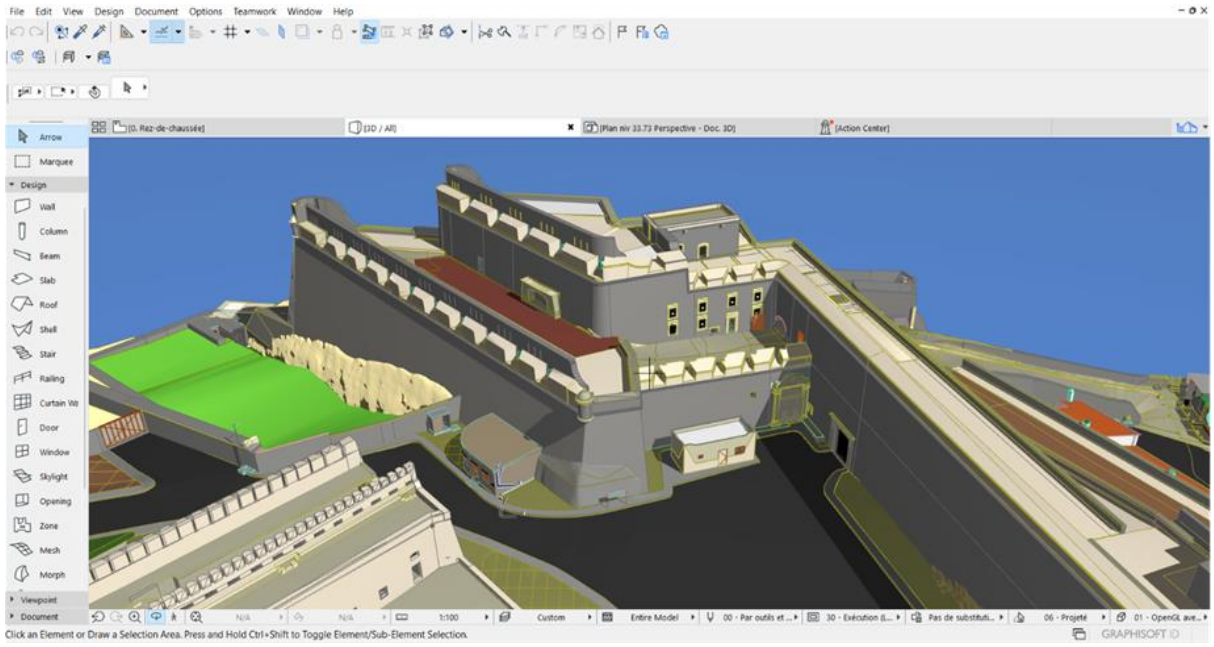

Figure 9. HBIM model of the North-West Bastion produced in ArchiCAD.

Table 5. Modeled object categories and attached condition data. Example identifier: BNO_W_023 (Bastion Nord-Ouest, wall, 023).

Element type	Modeling method	IFC class	Condition data attached
Curtain walls / ramparts	ArchiCAD wall / object	IfcWall	Cracking, dislocation, loss
Bastions, orillons, scarps	Custom object / morph	IfcBuildingElementProxy	Cracking, marine erosion
Vaults (barrel / groin)	Custom object / morph	IfcBuildingElementProxy	Cracking, deformation
Échauguettes (bartizans)	Custom object	IfcBuildingElementProxy	Cramp corrosion, collapse
Parapets (embrasures/loopholes)	Wall / object	IfcWall	Dislocation, loss
Slabs / terraces	Slab / object	IfcSlab	Cracking, leaching
Openings	Door / window / object	IfcDoor / IfcWindow	Damage code

Condition assessment: typology, coding, and severity

Condition was assessed on orthophotos and WebShare imagery and recorded in three coordinated instruments: a per-space condition assessment sheet describing each pathology and its cause; an entity-level crack register; and a synthesis report. Recommended interventions were recorded in a separate column annexed to the sanitary sheet — keeping diagnosis distinct from proposal (Table 8).

Pathology typology

The pathologies recorded correspond to recognized stone-deterioration families (ICOMOS-ISCS; Vergès-Belmin, 2008): structural cracking; dislocation and collapse of rubble (moellon) masonry; alveolization and pulverulence of carved/ashlar stone; leaching of joint mortars and renders; corrosion and expansion of metal cramps; marine erosion of the rock substrate; and biological colonization (Conocarpus erectus, Phoenix, Eriobotrya, Cestrum, Juniperus). Table 6 gives the coding.

Table 6. Condition-code families, mapped to ICOMOS-ISCS terms (codes illustrative of the project scheme).

Code	Pathology (ICOMOS-ISCS family)	Severity basis	Typical IFC carrier
FIS	Cracking / fissuration (fracture)	Penetration class (§3.7.3)	IfcWall / proxy
DIS	Dislocation / collapse of rubble masonry (detachment)	Extent / stability	IfcWall
ALV	Alveolization & pulverulence (material loss)	Depth / area	proxy / IfcWall
LES	Leaching of mortars & renders (loss)	Area / joint depth	IfcWall
AGR	Cramp corrosion & expansion (cracking/detachment)	Displacement	proxy
ERO	Marine erosion of rock substrate (erosion)	Rate / extent	site / proxy
BIO	Biological colonization (biological)	Cover / root action	IfcWall / site

The crack register

Each crack was given a unique reference keyed to the drawing on which it appears — by section and/or elevation, with its location, orientation (inclined, vertical, horizontal, or mixed), trace (simple or multiple), length (m), opening between lips (cm), and penetration class. Table 7 reproduces representative entries for the North-West Bastion.

Table 7. Representative entries from the North-West Bastion crack register (43 cracks in total).

Reference	Location	Orientation	Length	Opening	Penetration
Fis-Coupe BB-01	Outer face, embrasure	Vertical	4.67 m	3 cm	Deep
Fis-Coupe BB-04	Angle chain CA1	Inclined	7.47 m	2 cm	Partly through
Fis-Coupe BB-09	Upper east outer face	Inclined	17.32 m	2 cm	Partly through
Fis-Coupe DD-06	Outer face, bay surround	Vertical	4.80 m	3 cm	Deep
Fis-Ouest-04	Échauguette, south side	Vertical	10.20 m	1.5 cm	Deep
Fis-Nord-05	Échauguette, north side	Vertical	1.83 m	3.4 cm	Fully through

Severity scale and quantification

Cracks were graded on a four-level penetration scale — superficial < deep < partially through < fully through — combined with length and opening. For the North-West Bastion, the 43 catalogued cracks comprise 22 superficial (51%), 8 deep (19%), 12 partially through (28%), and 1 fully through (2%); thus ≈ 49% are deep or through-going and structurally significant, the longest reaching 17.32 m and the widest opening 3.4 cm.

BIM enrichment and the semantics of the model

Enrichment was governed by a single principle: the model must remain intelligible to a future conservator. Three choices give each element an unambiguous meaning (Bianchini et al., 2016; Quattrini et al., 2018; Valentini et al., 2023). First, identity: every element carries an entity-based identifier (e.g., BNO for the North-West Bastion), an IFC class, and a layer. Second, a controlled property structure separates two attribute groups that were previously conflated — condition (observed) and intervention (proposed). Third, interoperability: the model was exported in IFC 2x3 — the schema agreed with project partners — and validated in Tekla BIMsight to confirm that classifications were present, geometry preserved, and properties retained.

Table 8. Worked property set for one element, showing the deliberate separation of identity, condition, and intervention attributes.

Property (group)	Example value — element BNO_W_023
Element_ID (identity)	BNO_W_023
IFC_Type (identity)	IfcWall
Entity / Historical_Phase (identity)	North-West Bastion / Spanish period
Material (identity)	Rubble stone masonry (moellon)
Pathology_Code (condition)	Fis-Coupe BB-04
Pathology_Type (condition)	Inclined crack, angle chain CA1
Length / Opening (condition)	7.47 m / 2 cm
Severity_Penetration (condition)	Partially through
Recommended_Intervention (intervention)	Stitching + lime-grout injection; re-pointing with compatible mortar
Intervention_Status (intervention)	Proposed

Because condition and intervention are distinct attribute groups, the model answers conservator queries such as “list all elements with through-going cracks” or “select elements requiring stainless-steel cramp replacement,” without confusing a degradation map with an intervention indication (cf. Giannattasio et al., 2020; Ippolito et al., 2023).

Results

The integrated survey produced comprehensive coverage and queryable HBIM. Table 9 collects the headline figures; North-West Bastion values are measured, whereas site-wide element counts are approximate, pending completion of the model audit.

Table 9. Summary of results.

Result	Value
Site area documented	≈ 54,000 m²
TLS scans / HDR scans	3,000 / 1,200
GPS control stations	31 (with total-station network)
Survey duration	≈ 119 field-days over 13 months (access-restricted)
GPR profiles / key finding	10 profiles; probable buried vault (~1 m depth)
North-West Bastion cracks catalogued	43 (22 superficial, 8 deep, 12 partly through, 1 fully through)
Deep or through-going cracks (NW Bastion)	≈ 49%
Modeled elements (site)	≈ 5,000 (provisional)
Mean registration residual (in/out)	3 mm / 10 mm

Worked example: the North-West Bastion

The North-West Bastion illustrates the workflow end-to-end. From the registered cloud and WebShare imagery (Figure 7), the bastion — its curtain returns, orillon, parapets with embrasures, échauguettes, and vaulted casemates — was modeled in ArchiCAD (Figure 9) and enriched (Figure 8). Its condition assessment sheets, organized by elevation (West, North) and by level (+52.37, +53.93, +71.72, +78.37 m), record dislocation and collapse of rubble facing, alveolization of carved stone at the land gate, corrosion of metal cramps in the échauguettes, leaching of joint mortars, and partial échauguette collapse. The crack register catalogues 43 fissures (Table 7), 49% of them deep or through-going, the most severe being a fully-through vertical crack in the north échauguette (Fis-Nord-05) and a 17.32 m inclined crack on the upper east face (Fis-Coupe BB-09). Each finding is carried in

the model as a condition attribute, paired with but kept distinct from its recommended intervention (Table 8).

Conservation interpretation and recommended interventions

The recorded condition drives a conservation response consistent with minimum-intervention and material-compatibility principles: careful purging of unstable masonry; lime-grout injection and stitching of cracks; re-pointing and rendering with mortars matched to the existing in nature, granulometry, and tint (avoiding cementitious, impermeable materials); relancis — piecing-in of rubble and ashlar with identical stone; replacement of corroded cramps with 316L stainless steel; temporary shoring of embrasures; and consolidation/anchoring of the eroded rock substrate. Stored as proposals against each element, these make the model a maintenance and monitoring tool, not only a record.

Discussion

The integrated, TLS survey — disciplined by a total-station network and 31 GPS stations and supplemented by GPR — documented a 54,000 m² multi-period fortress to a quality suitable for modeling and condition mapping, despite the UAV prohibition and a fragmented, access-restricted schedule, provided inaccessible zones are explicitly accounted for. Embedding a coded condition assessment in an ArchiCAD HBIM, with identity, condition, and intervention held as distinct attribute groups and exported in validated IFC 2x3, produced a model that answers conservator queries rather than merely displaying geometry. The decisive adaptations were the entity-based division carried through every phase, the substitution of archival and adjacent-TLS data for prohibited aerial coverage, the use of GPR to probe the inaccessible subsurface, and the acceptance of manual modeling effort spread over a long access-constrained campaign.

Beyond demonstrating feasibility, the condition record carries interpretive weight for the conservation of the fortress. That roughly half of the forty-three fissures catalogued in the North-West Bastion penetrate deeply or pass through the masonry section indicates that degradation is not confined to surface weathering but has reached the load-bearing fabric, with the longest fracture (17.32 m) and the widest opening (3.4 cm) concentrated on the exposed outer faces and the échauguettes. Considered together with the recorded dislocation of rubble facing, the alveolization of carved stone, the leaching of joint mortars, and the corrosion-driven expansion of metal cramps, the pattern points to the superposition of structural movement and marine-driven material loss rather than to a single dominant mechanism. Recording this distribution at entity level and grading it by penetration converts the documentation from a descriptive inventory into a triage instrument, allowing elements to be ranked by structural significance and interventions to be sequenced accordingly, in keeping with the minimum-intervention and material-compatibility principles that govern the proposed treatments.

Two features distinguish the present workflow from routine scan-then-model practice. First, the integration of ground-penetrating radar extends the record below the visible surface: the two interconnected anomalies interpreted as a probable buried vault are at once a heritage-value finding and a conservation-risk indicator, and — although they require coring or excavation to confirm — they show how subsurface prospection can be folded into a documentation campaign so that what is concealed is registered alongside what is measured. Second, the explicit separation of observed condition from proposed intervention as distinct attribute groups addresses a recurrent ambiguity in semantic HBIM, in which a degradation map and an intervention indication are too readily conflated (Bianchini et al., 2016; Giannattasio et al., 2020; Quattrini et al., 2018; Ippolito et al., 2023). Holding the two apart, and binding each to a stable entity identifier and IFC class, lets the model be interrogated for conservation decisions — isolating, for instance, all through-going cracks or all elements awaiting stainless-steel cramp replacement — and re-interrogated as the fabric evolves, so that the HBIM operates as a maintenance and monitoring instrument rather than a static deliverable (Chelaru et al., 2024).

The broader value of the study lies in its transferability to settings where the conditions assumed in much of the documentation literature do not hold. Where aerial survey is prohibited, trained personnel and instrumentation are scarce, and access is intermittent, the decisive choices proved to be organizational rather than instrumental: a fixed division into survey entities maintained across every phase, a topographic control framework that bounded error propagation across a thirteen-month campaign, and the deliberate substitution of archival and adjacent-station data for coverage that could not be acquired. These choices carry a cost that should not be understated. The condition assessment rests on the visual interpretation of orthophotos and panoramic imagery rather than on instrumented diagnostics; the modeling of irregular fabric remains manual and therefore exposed to operator

variability; and the site-wide element counts are, as reported, still provisional. Such constraints bound the strength of the present claims, yet they also delineate a realistic and reproducible standard for the condition-oriented documentation of large, access-constrained defensive heritage in comparable contexts (Georgopoulos et al., 2020; Mancuso & Pasquali, 2016; Sarmiento et al., 2019).

Consistent with Rocha et al. (2020), the Scan-to-BIM process remained largely manual; it appears to reduce field-documentation time relative to conventional manual survey, although no formal time-motion comparison was performed. The results align with large-scale TLS campaigns on complex fortifications (Pritchard et al., 2017; Sarmiento et al., 2019) and with semantic-HBIM practice (Bianchini et al., 2016; Quattrini et al., 2018; Valentini et al., 2023). No methodological novelty in TLS itself is claimed; the contribution is the disciplined integration of techniques and the condition-to-HBIM semantics under real operational constraints.

Challenges and mitigation strategies

The campaign was shaped by several operational and environmental constraints intrinsic to the documentation of an active, multi-period defensive complex. Each is examined below in terms of its underlying cause, its concrete consequence for the survey, and the mitigation adopted.

The most pervasive constraint was restricted and intermittent access. Because Mers-el-Kébir remains an active military installation, entry was authorized only within discontinuous windows negotiated sector by sector. The immediate consequence was a fragmented, 13-month campaign in which acquisition could neither proceed continuously nor follow an optimal spatial sequence. This was mitigated through sector-based scheduling aligned with the authorized windows and, decisively, by tying every sector to a common reference frame through a total-station network and 31 GPS control stations, so that sectors surveyed weeks or months apart could be registered together without accumulating drift.

A second constraint was the prohibition of unmanned aerial vehicle (UAV) survey. Military regulation precluded any aerial acquisition, which would otherwise have been the natural means of recording roofs, upper parapets, and the sea-facing facades. The resulting deficit in the coverage of high and seaward surfaces was offset by extending terrestrial laser scanning from elevated and adjacent stations and by recourse to archival documentation, while recognizing explicitly that a residual set of inaccessible zones persists and must be accounted for in any metric interpretation.

The scale of the acquisition imposed a heavy computational load. A site of approximately 54,000 m² captured at high resolution yields point clouds whose aggregate volume exceeds the capacity of routine workstation processing when handled as a single dataset. The survey therefore adopted an entity-based processing strategy, partitioning the complex into the survey entities defined at the outset and exporting each as a separate, decimated E57 set kept under 5 GB, which preserved tractable file sizes without compromising the common georeferencing.

Finally, the modeling phase remained predominantly manual. The morphological irregularity of historic fabric — deformed vaults, battered scarps, eroded rock, and non-standard mouldings — is poorly served by parametric BIM libraries and resists automation, rendering the work time-consuming and susceptible to operator variability. This was mitigated by carrying the entity division into the modeling environment so that operators could work in parallel within a shared framework, by enforcing consistent identifiers, layers, and IFC classes, and by validating the federated model in Tekla BIMsight to confirm that classifications, geometry, and property sets were preserved.

These constraints and their corresponding responses are summarized in Table 10.

Table 10. Principal limitations, impacts, and mitigation strategies.

Limitation	Cause	Impact	Mitigation
Restricted, intermittent access	Active military site	13-month fragmented campaign	Sector-based scheduling; 31 GPS control points
UAV not permitted	Military restriction	Reduced roof / sea-facing coverage	TLS + archival records
High computational load	Large point cloud	Entity-based processing	E57 per-entity export

Limitation	Cause	Impact	Mitigation
Manual modeling	Irregular geometry; no automation	Time-consuming; operator variability	Entity division + standards + Tekla validation

Conclusion

Consistent with prior large-scale campaigns on complex fortifications (Pritchard et al., 2017; Sarmiento et al., 2019), this study shows that an integrated, TLS-led Scan-to-HBIM survey of a large, multi-period fortress is feasible under military access restrictions. What was done: a 54,000 m² fortress was documented by an integrated survey (manual, total station with 31 GPS control stations, photography, TLS, GPR) over a 13-month access-restricted campaign of 3,000 scans (1,200 HDR), registered and modeled as a semantically structured HBIM in ArchiCAD, with condition data exported in validated IFC 2x3. What was produced: a high-resolution point cloud, orthophotos, a queryable HBIM linking identity, condition, and recommended intervention, a GPR-based indication of a probable buried vault, and a quantified condition record (for the North-West Bastion, 43 catalogued cracks, ≈ 49% structurally significant). Limitations remain: the manual modeling effort, the visual basis of the condition assessment, and the zones uncovered by the UAV prohibition. Future work should pursue greater automation for irregular fabric, the integration of instrumented diagnostics (moisture, structural monitoring, and verification of the GPR anomalies), and a low-cost workflow suited to regional conservation practice.

More broadly, the study offers a replicable template for documenting heritage that is at once large, stratified, and operationally constrained — a combination characteristic of military and coastal defensive sites across North Africa and the wider Mediterranean, yet under-represented in the Scan-to-HBIM literature. By showing that a disciplined, control-anchored, multi-technique survey can yield a semantically structured and queryable conservation model without aerial coverage or extensive automation, it lowers the threshold for institutions working under comparable constraints to move from manual survey and CAD drafting toward information-rich documentation. Realizing that potential at scale will depend less on new sensing hardware than on consolidating such workflows, and the shared conventions for condition coding and interoperability that underpin them into a maintainable and regionally transferable practice.

Acknowledgements

The authors extend their deepest gratitude to the GAMAP Group (S.C.P.A. ARCHIMED and BET ALI PACHA Mehdi), where all the work was done with their team (The group is based in Algiers, Algeria). Their invaluable expertise in Laser scanning, 3D modeling, and condition assessment proved instrumental in pursuing and achieving this research project. The team's solid support, coupled with their generous permission to share and publish the results of our joint effort, significantly contributed to the successful completion of this study. We entirely acknowledge and appreciate their role in our research project.

References

[01] Alshawabkeh, Y., Baik, A., & Miky, Y. (2024). HBIM for conservation of built heritage. ISPRS International Journal of Geo-Information, 13(7), 231. https://doi.org/10.3390/ijgi13070231

[02] Aricò, M., Ferro, C., La Guardia, M., Lo Brutto, M., Taranto, G., & Ventimiglia, G. M. (2024). Scan-to-BIM process and architectural conservation: Towards an effective tool for the thematic mapping of decay and alteration phenomena. Heritage, 7(11), 6257–6281. https://doi.org/10.3390/heritage7110294

[03] Avena, M., Patrucco, G., Remondino, F., & Spanò, A. (2024). A scalable approach for automating scan-to-BIM processes in the heritage field. The International Archives of the Photogrammetry, Remote Sensing and Spatial Information Sciences, XLVIII-2/W4-2024, 25–31. https://doi.org/10.5194/isprs-archives-XLVIII-2-W4-2024-25-2024

[04] Bianchini, C., Inglese, C., & Ippolito, A. (2016). Il contributo della Rappresentazione nel Building Information Modeling (BIM) per la gestione del costruito. DISEGNARECON, 9(16), 101–109.

[05] Boardman, C., Bryan, P., McDougall, L., Reuter, T., Payne, E., Moitinho, V., Rodgers, T., Honkova, J., O'Connor, L., & Blockley, C. (2018). 3D laser scanning for heritage: Advice and guidance on the use of laser scanning in archaeology and architecture (3rd ed.). Historic England.

[06] Brumana, R., Banfi, F., Cantini, L., Previtali, M., & Della Torre, S. (2019). HBIM level of detail-geometry-accuracy and survey analysis for architectural preservation. The International Archives of the Photogrammetry, Remote Sensing and Spatial Information Sciences, XLII-2/W11, 293–299. https://doi.org/10.5194/isprs-archives-XLII-2-W11-293-2019

[07] Cámara, A. (Ed.). (2010). Leonardo Turriano, ingeniero del rey. Fundación Juanelo Turriano.

[08] Chelaru, B., Onuțu, C., Ungureanu, G., & Şerbănoiu, A. A. (2024). Integration of point cloud, historical records, and condition assessment data in HBIM. Automation in Construction, 161, 105347. https://doi.org/10.1016/j.autcon.2024.105347
[09] Cormontaigne, L. de. (1741). Architecture militaire, ou l'art de fortifier [Treatise]. Bibliothèque nationale de France, Gallica (ark:/12148/bpt6k1512672t).
[10] De Castro, J. J. (2004). Los ingenieros reales de los Reyes Católicos: Su nuevo sistema de fortificación. In A. Valdés (Ed.), Artillería y fortificaciones en la Corona de Castilla durante el reinado de Isabel la Católica 1474–1504 (pp. 320–383). Madrid.
[11] Dell'Amico, A., Sanseverino, A., & Albertario, S. (2024). Point cloud data semantization for parametric scan-to-HBIM modeling procedures. In A. Giordano, M. Russo, & R. Spallone (Eds.), Beyond digital representation: Digital innovations in architecture, engineering and construction. Springer. https://doi.org/10.1007/978-3-031-36155-5_33
[12] Epalza, M., Vilar, J., & Villanueva, J. (1988). Planos y mapas hispánicos de Argelia, siglos XVI–XVIII (Vol. 1). Instituto Hispano-Árabe de Cultura.
[13] Escudero, P. A. (2023). Scan-to-HBIM: Automated transformation of point clouds into 3D BIM models for the digitization and preservation of historic buildings. VITRUVIO – International Journal of Architectural Technology and Sustainability, 8(2), 52–63. https://doi.org/10.4995/vitruvio-ijats.2023.20413
[14] Ferro, A., Lo Brutto, M., & Ventimiglia, G. M. (2023). A scan-to-BIM process for the monitoring and conservation of the architectural heritage: Integration of thematic information in an HBIM model. The International Archives of the Photogrammetry, Remote Sensing and Spatial Information Sciences, XLVIII-M-2-2023, 549–556. https://doi.org/10.5194/isprs-archives-XLVIII-M-2-2023-549-2023
[15] Georgopoulos, A., Skamantzari, M., & Tapinaki, S. (2020). Digitally developing medieval fortifications. Editorial Universitat Politècnica de València, 317–324
[16] Giannattasio, C., Papa, L. M., D'Agostino, P., & D'Auria, S. (2020). The BIM model for existing building heritage: From the geometric data acquisition to the information management. In L. Agustín-Hernández, A. Vallespín Muniesa, & A. Fernández-Morales (Eds.), Graphical heritage (pp. 311–322). Springer. https://doi.org/10.1007/978-3-030-47979-4_28.
[17] Ippolito, A., Attenni, M., & Darwa, R. (2023). HBIM as a tool for heritage presentation of Santa Maria in Trastevere. SCIRES-IT – SCIentific RESearch and Information Technology, 13(1), 53–66. https://doi.org/10.2423/i22394303v13n1p53
[18] Jerushan J., Kevin Enoch, Vincent Sam Jebadurai S., Hemalatha G., Arunraj E., Ringle Raja S., Nirmala T., Brindha D. (2024). Integrating scan data to enhance BIM: An overview of techniques, mapping strategies and building life-cycle applications. Przegląd Elektrotechniczny, 2024(10). https://doi.org/10.15199/48.2024.10.17
[19] Jia, S., Liao, Y., Xiao, Y., Zhang, B., Meng, X., & Qin, K. (2022). Methods of conserving and managing cultural heritage in classical Chinese royal gardens based on 3D digitalization. Sustainability, 14(7), 4108. https://doi.org/10.3390/su14074108
[20] Lasheras Merino, F., & Niar, S. (2015). Estudio del sistema defensivo de Orán. In International Conference on Modern Age Fortifications of the Western Mediterranean Coast (FORTMED 2015) (pp. 251–256).
[21] Malihi, S., & Bosché, F. (2024). Integrating surface-related indicators of coverage, distance and distribution for quantifying scan-to-BIM confidence level. ISPRS Annals of the Photogrammetry, Remote Sensing and Spatial Information Sciences, X-4/2024, 223–229. https://doi.org/10.5194/isprs-annals-X-4-2024-223-2024
[22] Mancuso, A., & Pasquali, A. (2016). St. Giovanni Tower on the Elba Island: Survey and analysis for a digital comprehension. In Defensive architecture of the Mediterranean, XV to XVIII centuries (p. 257).
[23] Nowak, R., Orłowicz, R., & Rutkowski, R. (2020). Use of TLS (LiDAR) for building diagnostics with the example of a historic building in Karlino. Buildings, 10(2), 24. https://doi.org/10.3390/buildings10020024
[24] Pestemaldjoglou, A. (1940). Mers-el-Kébir, historique et description de la forteresse. Revue Africaine, 84, 154–185.
[25] Pritchard, D., Sperner, J., Hoepner, S., & Tenschert, R. (2017). Terrestrial laser scanning for heritage conservation: The Cologne Cathedral documentation project. ISPRS Annals of the Photogrammetry, Remote Sensing and Spatial Information Sciences, IV-2/W2, 213–220. https://doi.org/10.5194/isprs-annals-IV-2-W2-213-2017
[26] Pritchard, D., Rigauts, T., Ripanti, F., Ioannides, M., Brumana, R., Davies, R., Avouri, E., Cliffen, H., Joncic, N., Osti, G., & Toumpouri, M. (2021). Study on quality in 3D digitisation of tangible cultural heritage. In Proceedings of ARQUEOLÓGICA 2.0 & GEORES 2021. Universitat Politècnica de València. https://doi.org/10.4995/arqueologica9.2021.12113
[27] Quattrini, R., Battini, C., & Mammoli, R. (2018). HBIM to VR: Semantic awareness and data enrichment interoperability for parametric libraries of historical architecture. The International Archives of the Photogrammetry, Remote Sensing and Spatial Information Sciences, XLII-2, 937–943. https://doi.org/10.5194/isprs-archives-XLII-2-937-2018
[28] Rocha, G., Mateus, L., Fernández, J., & Ferreira, V. (2020). A scan-to-BIM methodology applied to heritage buildings. Heritage, 3(1), 47–67. https://doi.org/10.3390/heritage3010004.
[29] Roman, O., Avena, M., Farella, E. M., Remondino, F., & Spanò, A. (2023). A semi-automated approach to model architectural elements in scan-to-BIM processes. The International Archives of the

Photogrammetry, Remote Sensing and Spatial Information Sciences, XLVIII-M-2-2023, 1345–1352. https://doi.org/10.5194/isprs-archives-XLVIII-M-2-2023-1345-2023

[30] Sarmiento, J. C., Bercero, A. M., Jimenez, D. L., Fernandez, J. C., & Garcia-Almirall, P. (2019). Large scale project architectural surveys. IOP Conference Series: Materials Science and Engineering, 471(8), 082045. https://doi.org/10.1088/1757-899X/471/8/082045

[31] Stylianidis, E. & Remondino, F. (2016). 3D recording, documentation and management of cultural heritage. Whittles Publishing

[32] Suchocki, C., Błaszczak-Bąk, W., Damięcka-Suchocka, M., Jagoda, M., & Masiero, A. (2020). On the use of the OptD method for building diagnostics. Remote Sensing, 12(11), 1806. https://doi.org/10.3390/rs12111806

[33] Tini, M. A., Forte, A., Girelli, V. A., Lambertini, A., Roggio, D. S., Bitelli, G., & Vittuari, L. (2024). Scan-to-HBIM-to-VR: An integrated approach for the documentation of an industrial archaeology building. Remote Sensing, 16(15), 2859. https://doi.org/10.3390/rs16152859

[34] Valentini, M., Battini, C., & Vecchiattini, R. (2023). HBIM to support the executive design of a restoration: Critical issues related to geometric and semantic modeling. SCIRES-IT – SCIentific RESearch and Information Technology, 13(2), 125–136.

[35] Vergès-Belmin, V. (Ed.). (2008). Illustrated glossary on stone deterioration patterns (Monuments and Sites No. 15). ICOMOS – International Scientific Committee for Stone (ISCS).